Construction of Viscoelastic Biocompatible Films via the Layer-by-Layer Assembly of Hyaluronan and Phosphorylcholine-Modified Chitosan

Piotr Kujawa,[†] Gregory Schmauch,[†] Tapani Viitala,[§] Antonella Badia,[‡] and Françoise M. Winnik*[,†,‡]

Faculté de Pharmacie and Département de Chimie, Université de Montréal, C.P. 6128 Succursale Centre-Ville, Montréal, Quebec H3C 3J7, Canada, and KSV Instruments Ltd., Höyläämötie 7, 00380 Helsinki, Finland

Received June 6, 2007; Revised Manuscript Received July 15, 2007

Films of hyaluronan (HA) and a phosphorylcholine-modified chitosan (PC−CH) were constructed by the polyelectrolyte multilayer (PEM) deposition technique and their buildup in 0.15 M NaCl was followed by atomic force microscopy, surface plasmon resonance spectroscopy (SPR), and dissipative quartz crystal microbalance (QCM). The HA/PC−CH films were stable over a wide pH range (3.0−12.0), exhibiting a stronger resistance against alkaline conditions as compared to HA/CH films. The loss and storage moduli, G' and G'', of the films throughout the growth of eight bilayer assemblies were derived from an impedance analysis of the QCM data recorded in situ. Both G' and G'' values were one order of magnitude lower than the moduli of HA/CH films. The fluid gel-like characteristics of HA/PC−CH multilayers were attributed to their high water content (50 wt %), which was estimated by comparing the surface coverage values derived from SPR and QCM measurements. Given the versatility of the PEM methodology, HA/PC−CH films are attractive tools for developing biocompatible surface coatings of controlled mechanical properties.

Introduction

The polyelectrolyte multilayer (PEM) deposition technique,[1] whereby two or more oppositely charged water-soluble polymers are alternatively adsorbed onto a substrate, offers facile means of modifying the surfaces of metals, ceramics, plastics, or glass. The utility of PEM films derives from the flexibility of their design and from the ease of their fabrication with large scale conformity and uniformity of coverage. The applications of PEM films encompass many areas of materials science, including photonic, electrochemical, and separation devices.[2] The PEM deposition has also become a well-established methodology in clinical applications that require biomaterials with finely engineered surfaces, such as implant materials, stents, prostheses, and artificial organs. In these systems, the PEM films mediate the cellular responses upon device implantation, control processes such as inflammation and tissue regeneration, and modulate adhesion, migration, and proliferation of cells.[3−7] The chemical composition, surface topography, and rheological characteristics of PEMs control their functions and their interactions in the biological milieu.[8,9] The topography of PEM can be viewed readily by in situ atomic force microscopy imaging. Quantitative evaluation of the mechanical properties of PEM is more difficult to achieve. The Young moduli of various PEMs have been measured by nanoindentation with an atomic force microscopy tip or a colloidal particle deposited on a cantilever tip,[10−12] or alternatively via detection of stress-induced mechanical buckling instabilities.[13] Piezo-rheometric determinations give access to the complex shear modulus of PEMs up to 10−100 μm in thickness.[14] The elastic modulus and tensile strength of self-supporting polyelectrolyte membranes were also determined using a micromechanical analysis system[15] and microinterferometry.[16] Storage and loss moduli recorded by quartz crystal microbalance with dissipation have been reported for a number of PEMs.[17−19]

A variety of interacting macromolecules have been successfully employed for multilayer buildup, including synthetic polyelectrolytes and charged biopolymers, such as polysaccharides, enzymes, proteins, and nucleic acids.[3,7,20−23] We and others have assessed the use of PEMs consisting of the polysaccharides hyaluronan (HA) and chitosan (CH) in surface modifications of cardiovascular devices, intraocular implants, scaffolds for tissue engineering applications, and bucal drug delivery systems.[4,5,24−30] Hyaluronan, the simplest natural glycosaminoglycan, is a linear polyanion ($pK_a \approx 3.0$) consisting of alternating *N*-acetyl-β-D-glucosamine and β-D-glucuronic acid residues linked (1→3) and (1→4), respectively (Figure 1). It is involved in inflammation, atherosclerosis, restenosis, and metastasis.[31] Current clinical applications of HA in the biomedical field exploit its physical properties, in particular its natural tendency to form soft, highly hydrated, and nontoxic coatings, whereas more recent research trends focus on the exploitation of the intrinsic biological properties of HA.[32] The objectives then are to create biomacromolecular surfaces that can communicate with their host tissue and respond in a physiological manner.

Chitosan, a linear polycation composed of β-D-glucosamine and β-D−*N*-acetylglucosamine residues linked (1→4) (Figure 1), is obtained via deacetylation of chitin, a natural polysaccharide extracted from the exoskeleton of numerous arthropods.[33] It has found applications in biomedical engineering, tissue regeneration, drug delivery, and gene therapy. Chitosan dissolves readily in acidic aqueous solutions (pH < 6), but it is

* Author to whom correspondence should be addressed.
[†] Faculté de Pharmacie,Université de Montréal.
[‡] Département de Chimie, Université de Montréal.
[§] KSV Instruments Ltd.

10.1021/bm7006339 CCC: $37.00
Published on Web 09/13/2007

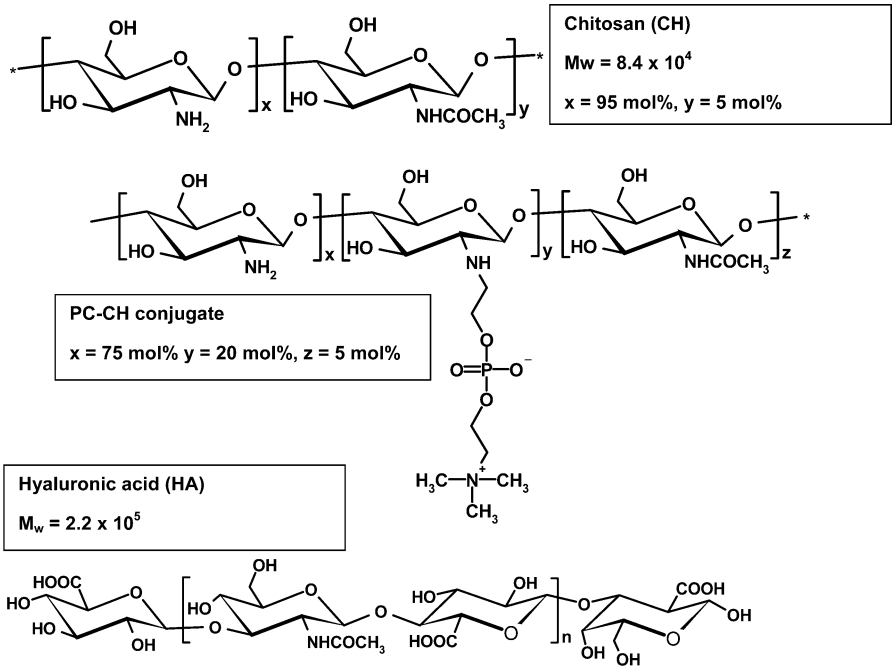

Figure 1. Idealized structure of the polyelectrolytes used in this study.

not soluble in water at neutral pH. Several strategies have been devised to prepare derivatives of CH that are soluble in neutral solutions while preserving the biocompatibility of chitosan. We recently reported the preparation of phosphorylcholine (PC)-modified chitosans, which proved to be nontoxic and soluble under physiological conditions, even with modest levels of PC incorporation (~20 mol % PC per glucosamine unit).[34] This modified chitosan is of particular interest for biomaterials applications in view of the remarkable protein-repelling properties and biocompatibility of PC-containing polymers.[35,36] Like chitosan, PC−CH (Figure 1) is a polycation under acidic conditions, but the properties of the two polymers are different, as a consequence of the conversion of a fraction of the CH primary amine groups ($pK_a \approx 6.5$) into secondary amines ($pK_a \approx 7.20$) upon covalent linkage of the PC groups.

In this study, we use atomic force microscopy (AFM), surface plasmon resonance spectroscopy (SPR), and dissipative quartz crystal microbalance (QCM) to monitor the growth of HA/PC−CH multilayers and to compare it with that of HA/CH multilayers. Since chitosan does not dissolve in solutions of pH > 6, the PEMs were prepared from polyelectrolyte solutions of pH 4.0, although PC−CH dissolves in solutions of neutral pH. Our study reveals that HA/PC−CH PEMs are stable over a broader pH window than HA/CH constructs, particularly in alkaline media. In addition, the phosphorylcholine substituents of chitosan affect the mechanical properties of the multilayers, which behave as soft fluidlike gels containing up to 50 wt % of water, in contrast to HA/CH films which contain less water (~15 wt %) and behave as hard solidlike gels.

Materials and Methods

Polyelectrolytes and Reagents. Hyaluronan (ARD, Pomacle, France, $M_w = 2.2 \times 10^5$ g mol^{-1} from light scattering analysis) and poly(ethyleneimine) (PEI, Aldrich, $M_w = 2.5 \times 10^4$ g mol^{-1} from light scattering data, as stated by the supplier) were used without further purification. 11-Mercaptoundecanoic acid (MUA, 95%, Aldrich) was recrystallized twice from hexane prior to use. Distilled water was deionized using a Milli-Q water purification system (Millipore). Chitosan was prepared by further deacetylation of a commercial sample (Wako-10, Wako Chemicals Co., degree of deacetylation (DDA) 85%, $M_n = 3.0 \times 10^4$ g mol^{-1}, $M_w = 8.4 \times 10^4$ g mol^{-1}), following a procedure reported previously.[34] The DDA of CH (95 mol %, relative to the number of saccharide units) was determined by ^{1}H NMR spectroscopy using a Bruker ARX-400 400 MHz spectrometer.[37] The phosphorylcholine-modified chitosan (PC−CH) was synthesized as reported previously. The degree of PC incorporation was 20 mol % PC, relative to the number of saccharide units, as determined by ^{1}H NMR spectroscopy and by a quantitative colorimetric phosphorus assay using an Agilent 8452A photodiode array spectrometer.[37]

The molecular weight of the polymers was measured by gel permeation chromatography (GPC) carried out on a GPC system consisting of an Agilent 1100 isocratic pump, a Dawn EOS multiangle laser light scattering detector (Wyatt Technology Co.), and an Optilab DSP interferometric refractometer (Wyatt Technology Co.). For analysis of the chitosans, the system was fitted with a TSK-GELPW (Tosoh Biosep, serial no. G0014) column eluted with a pH 4.5 acetic acid (0.3 M)/sodium acetate (0.2 M) buffer. For hyaluronan analysis, the system was fitted with a serial set of Shodex OH Pack SB-G and SP 806, 805, and 804 columns; eluent: aqueous 0.1 M $NaNO_3$/0.8 mM NaN_3; injection volume, 100 μL; flow rate: 0.5 mL min^{-1}; temperature, 25.0 °C. The refractive index increments ($\partial n/\partial c$) of the polymers were measured at 690 nm with the same refractometer used offline.

Assembly of Polyelectrolyte Multilayers. The polyelectrolyte multilayers were assembled following methods described previously[27] onto substrates cleaned prior to use by dipping in a piranha solution consisting of 70% concentrated sulfuric acid and 30% hydrogen peroxide, followed by copious rinsing with deionized water, and nitrogen drying. (**WARNING**: Piranha solution is extremely reactive and should be handled with extreme caution.) Solutions were prepared by direct dissolution of the polyelectrolytes in either aqueous NaCl (PEI or HA, 1.0 g L^{-1}, 0.15 M NaCl) or aqueous NaCl/acetic acid (CH or PC−CH, 1.0 g L^{-1}, 0.15 M NaCl/0.1 M CH_3COOH). The polyelectrolyte solutions' pH was adjusted to 4.0 (CH, PC−CH, and HA) or 8.0 (PEI) using aqueous concentrated HCl or NaOH solutions. Solutions of PC−CH were sonicated in a sonicator bath for 1 h prior to use. All polymer solutions were filtered through 0.45 μm Millipore PVDF filters prior to use. A self-assembled monolayer of MUA was prepared by incubating gold-coated LaSFN9 glass slides (50 nm Au, AFM experiments), gold-coated B270 glass slides (1 nm Ti/50 nm Au, Evaporated Metal Films, Ithaca, NY, SPR experiments) or gold-coated 5 MHz AT-

cut quartz crystals (Quartz Pro, Sweden, QCM experiments) into a MUA solution in ethanol (1 mM) for at least 12 h, followed by rinsing with ethanol and water. The MUA-modified gold surface was placed in a SPR or QCM fluid cell holder. The cell was filled with an aqueous PEI solution. After 20 min, it was flushed with 10 times the cell volume (~10 mL) of an aqueous NaCl solution (0.15 M, pH 4) to ensure removal of excess PEI. HA and CH (or PC−CH) were then successively deposited on the Au/MUA/PEI surface, beginning with HA, following the procedure described above for PEI. The build up process was continued up to 10 bilayers. Throughout the text, the term "layer" refers to a single polymer coating (HA, CH, or PC−CH), while the term "bilayer" is used to describe the assembly formed by a pair of oppositely charged polyelectrolytes. The nomenclature PEI−$(HA/CH)_k$ implies that the multilayer consists of k HA/CH bilayers deposited onto a substrate coated with PEI and that CH is the polyelectrolyte added last (topmost layer). The Au/MUA/PEI surface is defined as bilayer 0.

To assess the influence of a pH increase or decrease on the multilayer stability, PEI−$(HA/CH)_4$ or PEI−$(HA/PC-CH)_4$ films constructed at pH 4 in a QCM cell were treated with solutions of increasing pH values (from pH 6.0 to 11.0) or decreasing pH values (from pH 3.5 to 1.0) and constant ionic strength (0.15 M), followed by rinsing with an aqueous NaCl (0.15 M, pH 4.0) solution. Frequency shift versus time ($\Delta f-t$) curves were recorded to monitor the stability of the adsorbed multilayer upon addition of a solution of given pH value.

AFM Measurements. The AFM imaging was performed in tapping mode at ambient temperature with an extended Dimension 3100 scanning probe microscope and Nanoscope IIIa controller (Digital Instruments/Veeco). Multilayers were prepared directly in a custom-built Teflon liquid cell. To prevent any structural rearrangements of the film structure induced by jumps in the pH and/or ionic strength, each HA and CH deposition step was followed by a rinse with an aqueous NaCl solution of the same ionic strength (0.15 M) and pH (4.0) as the polyelectrolyte solutions, and all imaging was performed in the same NaCl solution. Images were acquired at various stages of the buildup. Surfaces were analyzed at the minimum applied force that would allow stable imaging using sharpened silicon nitride microlevers (model MSCT-AU, Veeco) with a typical radius of curvature of 20 nm, nominal spring constant of 0.1 N m^{-1}, and a resonance frequency of 7.55 kHz in liquid. The scan rate and image resolution used were 1 Hz and 512 × 512 pixels, respectively. Several macroscopically separated areas of the multilayer films were examined, and representative height images are presented. The reported widths are those measured at half-height. Unless otherwise mentioned, root-mean-square (rms) surface roughness analyses were carried out on 7.5 μm × 7.5 μm scans using the Nanoscope software. Images used for rms roughness analyses and film thickness measurements were corrected for bow/tilt by a third-order plane fit correction.

SPR Measurements. SPR measurements were carried out with a computer-controlled SR7000 SPR instrument (Reichert, Inc., Depew, NY) and a National Instruments Labview interface (SR7000 Alpha Instrument, version 2.24) for data acquisition and transfer. The instrument was equipped with a flow-through cell with a volume of ~1 mL and a surface area of 12 mm^2 , an injector port, a six-way low-pressure solvent selection valve, and a syringe pump (model PHD 2000, Harvard Apparatus). Surface plasmons were excited at the metal/solution interface in the Kretschmann configuration[38] using the p-polarized output from a GaAlAs laser (15 mW, 780 nm) and a hemicylindrical sapphire prism ($\epsilon = 1.7607$). The TM-polarized incident light was focused through the sapphire prism onto the underside of a gold-coated glass slide with an angular distribution of ~21°. The gold surface area irradiated is ~1 mm × 1.5 mm. Light totally internally reflected from the gold/solution interface was detected with a 3696-pixel CCD linear array for which the optical pixel signals were digitized with a 14-bit analogue-to-digital converter. Reflected light intensity versus pixel number spectra (referred to as "array scans") were generated by scanning the array detector. The SPR minimum pixel was tracked with time by a centroid algorithm using the signal from a few pixels on either side of the pixel of the lowest intensity value.

The shifts in the minimum pixel recorded during the deposition were converted to resonance angle changes ($\Delta\Theta_m$) using the pixel-to-incident angle relation, i.e., 1 pixel = 0.00513°, established through calibration of the SR7000 instrument across the refractive index range of ~1.33−1.38 with pure water and aqueous solutions of ~4−50 wt % ethylene glycol. To calculate the film thickness (d_f), the Fresnel modeling software Winspall (version 2.20) was used. The changes in resonance angle position $\Delta\Theta_m$ were fit using a six-layer model incorporating the sapphire prism ($n = 1.7607$), glass slide ($n = 1.5113$), Ti layer ($n = 2.7683$, $k = 3.3065$, $d = 1$ nm), Au layer ($n = 0.174$, $k = 4.86$, $d = 50$ nm), polymer film (n_f and d_f unknown), and buffer solution ($n_s = 1.333$). It is generally not possible to determine both n_f and d_f for an adsorbed, thin organic film from a single SPR curve. Any number of different combinations of n and d can produce the same $\Delta\Theta_m$ values. Thus, to obtain film thickness from $\Delta\Theta_m$, the film index of refraction must be known. The values of index of refraction employed were 1.3748 for the PEI layer, 1.3798 for the HA-terminated layers, and 1.3780 for the CH- or PC−CH-terminated layers, as determined earlier for HA/CH coatings.[27] The surface coverage Γ (expressed in ng/cm^2) was calculated using the relation

$$\Gamma = d_f(n_f - n_s)/(\partial n/\partial c) \quad (1)$$

where $\partial n/\partial c$ is the refractive index increment of polymers in solution.

QCM Measurements. A KSV QCM-Z500 (KSV Instruments, Helsinki, Finland) was used to monitor multilayer buildup. The QCM-Z500 instrument measuring principle is based on impedance analysis.[39] The quartz crystal is swept with potential perturbations of different frequencies close to the quartz crystal resonance frequency. The potential over the crystal and the current flowing through the crystal are recorded. This sweep is done as a function of time enabling the measurement of mass changes occurring on the quartz crystal electrode surface. Both the bulk liquid phase and the layer adsorbed on the crystal create mechanical perturbations on the crystal and changes of its electrical characteristics. The mechanical properties of the adsorbed layer can be determined by measuring the impedance of the crystal and using the transmission line model.[40] Knowing the resistance, inductance, and capacitance of the crystal, the frequency change of the crystal (Δf) and the dissipation (ΔD) can be calculated using an equivalent circuit analysis. If the layer adsorbed on the crystal surface is rigid and homogeneous, then the frequency changes recorded for the fundamental frequency of the crystal superimpose with the signals recorded for the higher harmonics and the frequency shift is proportional to the mass of the adsorbed material. Under this situation, the Sauerbrey eq 2 derived for rigid films can be applied

$$\Delta f = -N\frac{\Delta m}{C_f} \quad (2)$$

where C_f is the mass-sensitivity constant and $N = 1, 3, 5...$ is the overtone number.

However, when the added mass is soft and not fully coupled with the crystal oscillations, there are energy losses (or dissipation) in the system, a situation detected experimentally by the fact that the Δf values measured for different overtones do not overlap. The total impedance must then be treated as a nonlinear combination, represented by the following equation

$$Z_s = Z_s^{film}\left[\frac{Z_s^{liquid}\cosh(\gamma d_f) + Z_s^{film}\sinh(\gamma d_f)}{Z_s^{film}\cosh(\gamma d_f) + Z_s^{liquid}\sinh(\gamma d_f)}\right] \quad (3)$$

where Z_s^{film} is the mechanical impedance of the viscoelastic film, Z_s^{liquid} is the mechanical impedance of a Newtonian liquid, d_f is the film thickness, and γ is the complex wave propagation, which are given by the following expressions

$$Z_s^{film} = (G\rho_f)^{1/2} \quad (4)$$

$$Z_s^{liquid} = \left(\frac{\omega\rho_{liquid}\eta_{liquid}}{2}\right)^{1/2}(1+j) \quad (5)$$

$$\gamma = j\omega\left(\frac{\rho_f}{G}\right)^{1/2} \quad (6)$$

G is the complex shear modulus of the viscoelastic film defined by eq 7

$$G = G' + iG'' \quad (7)$$

where G' is the storage modulus and G'' is the loss modulus of the viscoelastic film, which is assumed to behave like a Voigt element. This assumption may be oversimplified, especially in the case of very soft, viscoelastic materials that resemble polymer solutions and reach Maxwellian features.[41] However, due to the limits in the precision of the QCM data, the introduction of additional fitting parameters into the model may be unreasonable. Thus, while one can easily make a comparison among the results of the fittings for various systems, the absolute values of G' and G'' should be taken only with limited confidence.

Equation 3 has several unknowns: the mass of the viscoelastic film and its storage and loss moduli. To solve for the unknown parameters, it is necessary to measure the response of the resonator for at least three overtone frequencies[40,42,43] ($N = 3$, 5, 7, and 9 in our case). The density (ρ_{liquid}) and viscosity (η_{liquid}) of the surrounding bulk liquid were taken as 1.004 g cm^{-3} and 0.903 mPa s for 0.15 M NaCl, respectively. All measurements were performed at 25.0 ± 0.1 °C.

Results and Discussion

AFM Imaging. The evolution of the HA/PC−CH and HA/CH multilayer topology and thickness during the assembly of up to 10 bilayers was monitored in situ by tapping mode AFM (Figure 2). Following the buildup of two HA/PC−CH bilayers upon a substrate coated with PEI, i.e., PEI−(HA/PC−CH)$_2$, the surface is covered with densely packed, isolated globular clusters, slightly elongated in shape, that are approximately 24 ± 6 nm in height and 255 ± 51 nm in length. The topology of a PEI−(HA/CH)$_2$ PEM built under the same conditions also presents globular features, but individual islets appear rounder than in the case of PEI−(HA/CH−PC)$_2$. Buildup of HA/CH constructs for up to six bilayers yields surfaces consisting of densely packed rounded globules reaching ~35 ± 8 nm in height. The rms roughness of the surface of PEI−(HA/CH)$_6$ is ~15 nm (Figure 3a). In the case of HA/PC−CH constructs, the vermiculate morphology, somewhat detectable in the two-bilayer construct, becomes the predominant feature of films consisting of six or more bilayers. For example, in the case of PEI−(HA/PC−CH)$_6$, the wormlike domains are on the order of 320 ± 35 nm across and 74 ± 14 nm in height. They grow to several microns in length upon further polyelectrolyte deposition (see bilayer 10 in Figure 2). The surface of the wormlike domains is rougher in the case of -PEI−(HA/PC−CH)$_{10}$ (rms roughness, 50 nm), as compared to PEI−(HA/CH)$_{10}$ (rms roughness, 35 nm, Figure 3a).

By repeatedly scanning a small area of a film under "hard" tapping conditions, it was possible to create holes in the nanocoatings. The ability to scrape off polymer from the substrate in the tapping mode was previously reported in the case of high molecular weight HA and CH constructs and taken as an indication of the loose association of the polyelectrolyte layers.[27] The thickness of films made with the HA/CH and HA/PC−CH pairs was measured throughout the construction. Scratching a PEI−(HA/CH)$_6$ film yields an average thickness of 120 nm ± 16 nm, while scratching a PEI−(HA/PC−CH)$_6$ film gives an average thickness of 200 nm ± 52 nm. The HA/PC−CH films were significantly thicker than their HA/CH

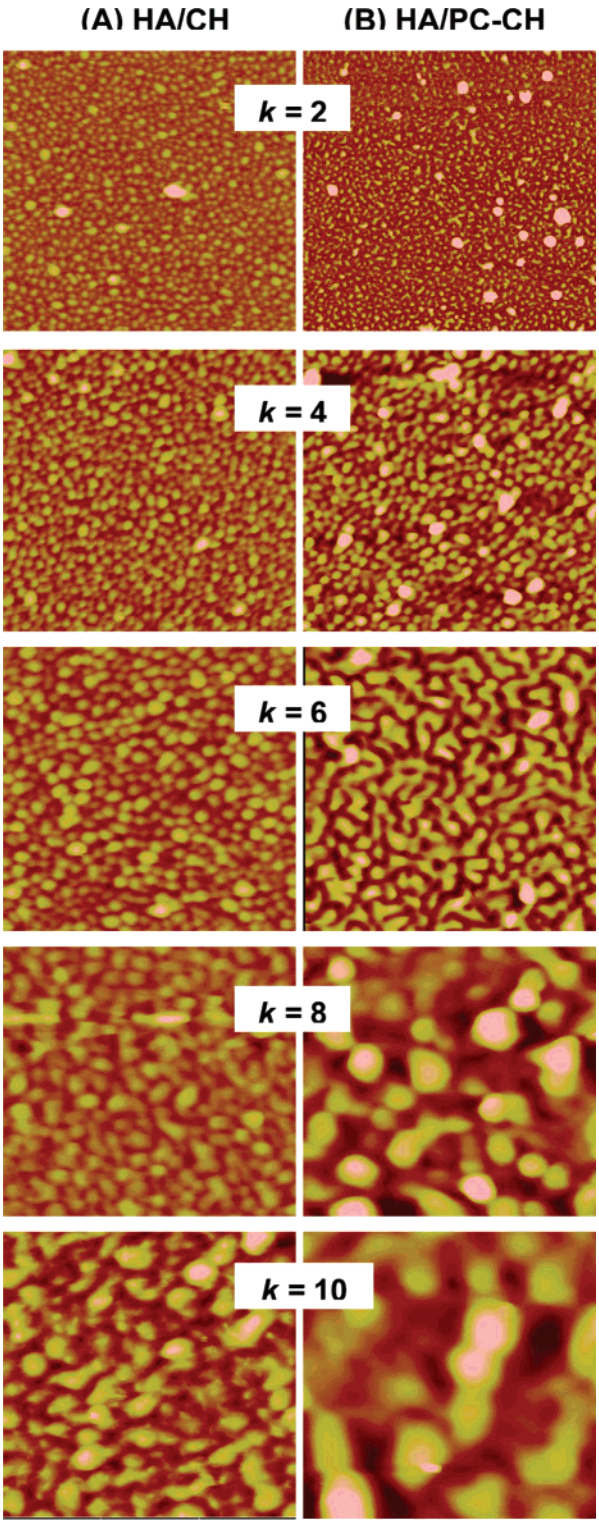

Figure 2. AFM topography images (7.5 μm × 7.5 μm) acquired in 0.15 M NaCl solution (pH 4.0) for different steps of the alternate deposition of (A) HA and CH and (B) HA and PC−CH onto a PEI-coated MUA−gold substrate. k indicates the number of HA/CH or HA/PC−CH bilayers. Maximum height or z-ranges are: (A) 150 nm (k = 2,4,6), 300 nm (k = 8, 10); (B) 50 nm (k = 2), 100 nm (k = 4,6), 150 nm (k = 8), and 250 nm (k = 10).

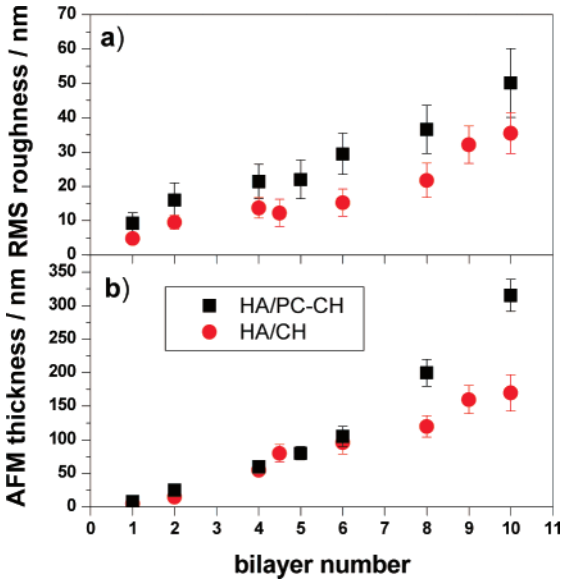

Figure 3. (a) Root-mean-square roughness and (b) multilayer thickness measured by AFM as a function of the number of HA/CH (red circles) and HA/PC−CH (black squares) bilayers.

counterparts throughout the build-up process after the deposition of the sixth bilayer (Figure 3b).

In summary, AFM imaging of $(HA/PC-CH)_k$ and $(HA/CH)_k$ multilayers at various stages of the deposition indicates that the HA/PC−CH films are rougher and thicker than HA/CH films (Figure 3). The HA/PC−CH multilayers adopt a vermiculate morphology in the early construction steps, i.e., after the deposition of the second bilayer, contrary to the case of HA/CH films for which rounded densely packed globules form preferentially, at least for constructs of up to eight bilayers. Much larger structures are present in the HA/PC−CH films, compared to HA/CH films, after the transition from globular to vermiculate topology.

SPR Characterization of PEM Buildup. The HA/PC−CH and HA/CH PEM deposition was monitored by in situ SPR, which allows one to determine the total film optical thickness after deposition of each polyelectrolyte and rinsing with aqueous NaCl. A five-layer optical model, described in the Materials and Methods section, was used in these calculations. Solvent trapped within the adsorbed layer does not contribute to its optical thickness, thus SPR provides a measure of the polymer contribution to the film mass (or "dry mass").[44] Plots of the changes in surface coverage as a function of the number of deposited bilayers for each polyelectrolyte pair exhibit a nonlinear or "exponential" growth pattern (Figure 4a). This PEM build up mechanism, whereby each bilayer formed by the polyanion/polycation pair is always thicker than the previous one, is characteristic of the HA/CH pair, at least under conditions of high ionic strength.[5,27] During the initial stage of PEM deposition, i.e., bilayers 1−3, the mass increment per deposition is small and of the same amplitude ($\sim 0.8 \pm 0.2$ μg/cm^2) for each construction step. As the buildup continues, the growth per bilayer becomes steeper. The mass gain per deposited polyelectrolyte layer reaches a value of $\sim 2.4 \pm 0.4$ μg/cm^2 under these conditions. The crossover between the two regimes occurs approximately after the deposition of the third bilayer for both polyelectrolyte pairs. Furthermore, the surface coverage at each step is the same for HA/PC−CH and HA/CH multilayers, in contrast to their thicknesses measured by AFM. Since the AFM scratch test yields the total thickness of the films, whereas SPR provides a measure of the polymer mass in the film, the discrepancy between the results of the two techniques must be taken as an indication of large differences in the degree of hydration of HA/CH and HA/PC−CH films.

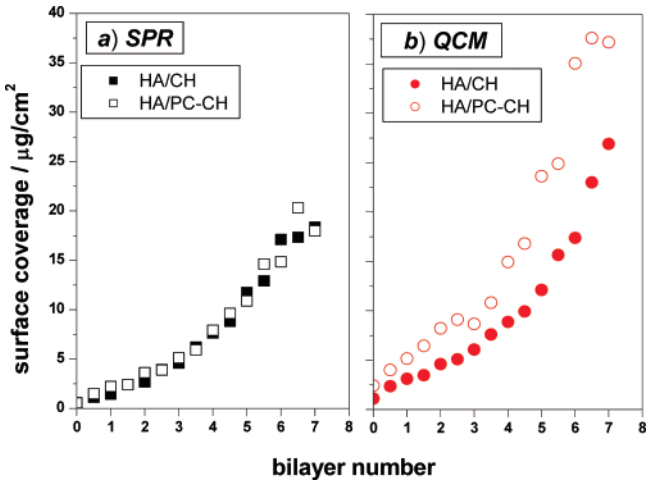

Figure 4. Surface coverage as a function of the number of bilayers during the alternate adsorption of HA and CH (filled symbols) or HA and PC−CH (open symbols) from 0.15 M NaCl (pH 4.0) aqueous polyelectrolyte solutions (1 g L^{-1}) onto a PEI-coated MUA−gold substrate monitored (a) by in situ SPR and (b) by dissipative QCM.

Dissipative QCM Characterization of PEM Deposition. In situ dissipative QCM analysis of the formation of HA/PC−CH and HA/CH multilayers onto a PEI-coated quartz crystal provides the total mass, polymer and water ("moving mass" or "wet mass"),[42−44] adsorbed on the crystal at each step of the PEM deposition. The evolution of the surface coverage recorded by QCM during the construction of eight bilayers of each polyelectrolyte pair is presented in Figure 4b. The exponential growth pattern exhibited by the SPR measurements (Figure 4a) is also observed under the PEM construction conditions of the QCM experiments. The surface coverage Γ follows an exponential dependence on the bilayer number (k),[45] $\Gamma = A \exp(\beta k)$, where the growth exponent β derived from QCM data is 0.339 ± 0.005 for HA/CH multilayers and 0.383 ± 0.006 for HA/PC−CH films (Figure S1 in the Supporting Information). Thus, for each bilayer, the wet mass of a HA/PC−CH bilayer is consistently larger than that of a HA/CH bilayer, corroborating the results of the AFM thickness assays (Figure 3). The difference between surface coverages recorded by QCM and by SPR for a given polyelectrolyte pair gives a measure of the degree of hydration of the PEMs.[42] We estimate that a PEI−$(HA/PC-CH)_7$ multilayer contains approximately 50 ± 15 wt % water, whereas a PEI−$(HA/CH)_7$ film has a water content of $\sim 15 \pm 7$ wt %. In both cases this value remains constant, within experimental uncertainty, throughout the buildup.

An important consequence of the high hydration level of HA/PC−CH PEMs is that they tend to behave as soft viscoelastic hydrogels rather than rigid films. The loss of film rigidity is readily detected via dissipative QCM measurements, whereas for solid films the frequency changes upon increasing film mass are the same for all overtones; in the case of viscoelastic gels, Δf versus time curves for different overtones do not superimpose. This feature is apparent in kinetic QCM traces recorded during the buildup of seven HA/PC−CH bilayers (Figure 5a). A deviation from rigid film behavior is detected already after the formation of the second bilayer, and it is amplified as the buildup proceeds. In the formation of HA/CH multilayers, however, it is only after the sixth bilayer deposition that the curves for each overtone cease to superimpose (Figure 5b),

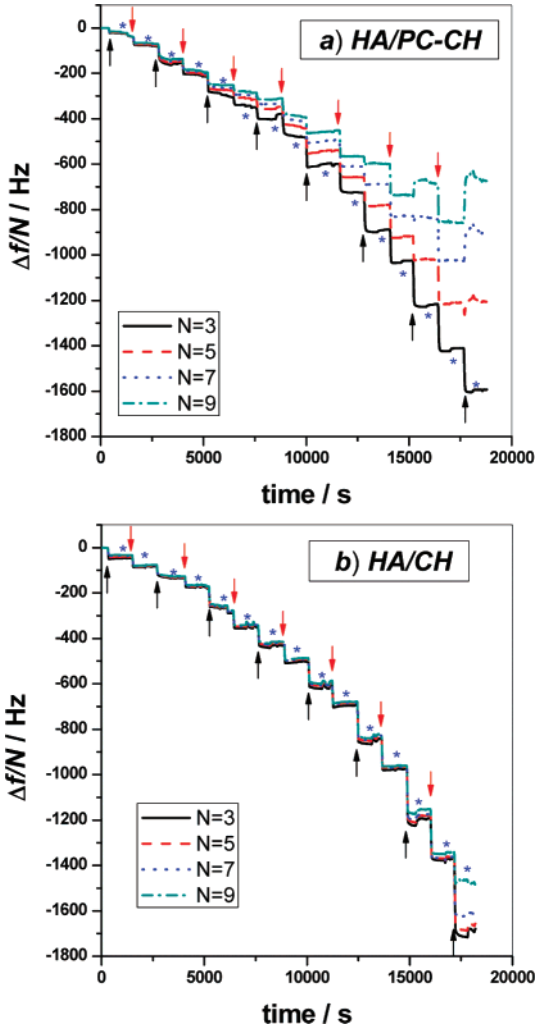

Figure 5. Frequency (Δf) as a function of time during the buildup of (a) HA/PC−CH and (b) HA/CH multilayers onto a MUA−gold-coated quartz crystal from 0.15 M NaCl (pH 4.0) aqueous polyelectrolyte solutions (1 g L^{-1}). The black arrows indicate the injections of polycations (PEI, CH, or PC−CH), the red arrows correspond to the injection of hyaluronan, and the blue stars point to the injection of an aqueous NaCl (0.15 M, pH 4.0) rinsing solution. Data are shown for four overtones.

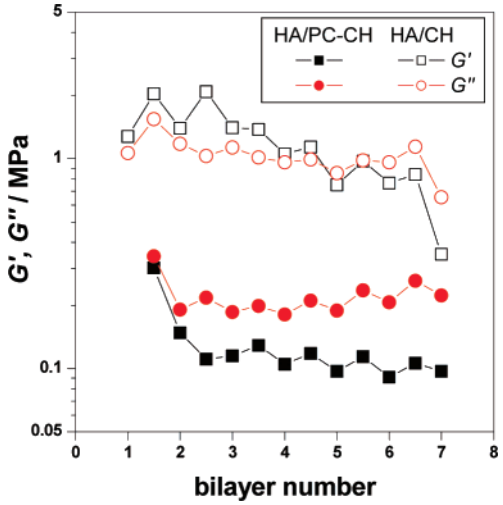

Figure 6. Storage modulus (G', square) and loss modulus (G'', circle) as a function of the number of bilayers during the alternate adsorption of HA and CH (open symbols) or HA and PC−CH (full symbols). Data were calculated from dissipative QCM data.

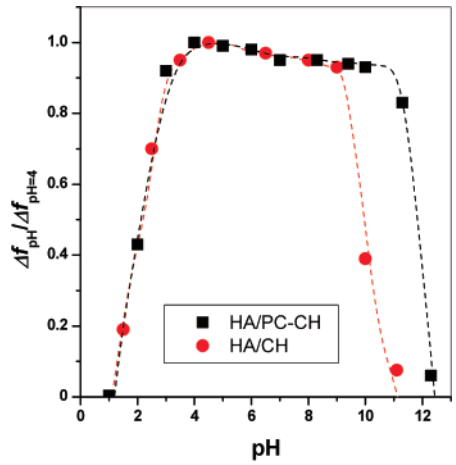

Figure 7. Changes in the relative frequency as a function of the pH of the contacting fluid for a four-bilayer construct of HA/PC−CH (full squares) and HA/CH (full circles) formed at pH 4.0 and subsequently treated with NaCl (0.15 M) solutions of different pH. The relative frequency shift was calculated as the ratio of the frequency shift for the fifth overtone measured for multilayers treated with a solution of a given pH to the frequency shift for the fifth overtone measured for multilayers kept in a fluid of pH 4.0.

vouching for the comparatively more rigid nature of HA/CH multilayers prepared in the conditions used here.

The total impedance values extracted from the QCM data recorded during deposition of the two pairs of polyelectrolytes was used to estimate the values of G' and G'', the storage and loss moduli, respectively, of the PEMs (see Figure S2 in the Supporting Information for the details of data fitting). Throughout the build up process, the values of G' and G'' recorded for HA/CH PEMs are nearly identical (1−2 MPa). These values are of the same order of magnitude as G' and G'' values of $(CH/HA)_{k>20}$ constructs derived from QCM experiments carried out under identical ionic strength conditions.[22] The G' and G'' values of the HA/PC−CH films (Figure 6) are lower by a factor of ~10, and the loss modulus is significantly higher than the storage modulus throughout the buildup. Although the evaluation of the storage and loss moduli from QCM data remains a subject of controversy, the trends observed, together with the AFM and SPR results, are indications that HA/PC−CH multilayers behave as fluid-like gels, whereas their HA/CH counterparts exhibit a more rigid gel-like behavior.

Stability of the Multilayers toward Changes in the pH of the Contacting Fluid. Films of four HA/CH or HA/PC−CH bilayers constructed with polyelectrolyte solutions of pH 4.0 (NaCl 0.15 M) in the QCM cell were contacted with solutions of increasing acidity, in one set of experiments, and with solutions of increasing basicity in another set. Changing the pH of the contacting solution from 4.0 to either 3.0 or 9.0 barely affected the frequency values recorded for each pair of polyelectrolytes, the original levels being nearly recovered upon exposure of the multilayer to a solution of pH 4.0 (Figure 7). Subjecting either a HA/CH or a HA/PC−CH multilayer to a solution of pH 2.5, however, resulted in a significant decrease of the frequency. This observation may signal partial polyelectrolyte desorption, corresponding to a decrease of the film thickness. One may envisage also that upon lowering the pH the multilayer shrinks and water is released into the contacting solution. These events would trigger a decrease of Δf in the QCM measurements. Lowering the contacting solution pH to 1.3 resulted in a further decrease of the frequency, which reached values recorded for a MUA−gold-coated quartz crystal, indicating a complete destruction of the film.

Increasing the solution pH value beyond 9.0 resulted in a sharp decrease of Δf in the case of HA/CH multilayers, but HA/PC−CH multilayers remained intact until the pH of the contacting solution exceeded 11.0. The disintegration of the multilayers in the high pH range is governed by a decrease of the ionization degree of chitosan.[30] Incorporation of PC modifies the pK_a of the chitosan polymer (pK_a = 7.20); thus the coatings become more stable in neutral and basic media. In contrast, the stability of the coatings within the low pH limit is governed by the ionization of hyaluronan, and consequently the resistance against strongly acidic fluids is approximately the same for both HA/CH and HA/PC−CH multilayers.

Conclusions

This study demonstrates that PC−CH, a weak polycation bearing a large number of zwitterionic groups, can interact with a weak polyanion (HA) to form robust films by the layer-by-layer process. Analysis of QCM data yielded information on the mechanical properties of the resulting films, which were shown to behave as highly hydrated soft gels. The high water content of HA/PC−CH films reflects the known ability of the phosphorylcholine group to undergo hydrogen bond interactions with water molecules. There have been several studies on the nanorheology of weak PEM assemblies, mostly for films composed of several hundreds of layers and a few micrometers in thickness. In general, it was observed that when the charge density of the coating is reduced, for example, by varying the pH of the polyelectrolyte solutions, the films adopt hydrogel-like properties with elastic moduli characteristic of soft viscoelastic materials and that the elastic moduli decrease as the coating thickness increases, possibly as a consequence of an increase in the water content of the films.[12] The facts that both storage and loss moduli for the HA/PC−CH coatings are ca. 1 order of magnitude smaller than those of HA/CH films and that G'' dominates the rheological response of the PC-containing system over the entire range of thickness probed are strong indications that their gel-like character and high water content are inherent characteristics as a result of the PC substituents. Our results also suggest means to modulate the viscoelasticity and hydrophilicity of HA/CH multilayers, for example, via construction of ternary films consisting of HA/CH and HA/PC−CH bilayers or by varying the degree of PC grafting onto chitosan. The versatility and ease of the PEM assembly, combined with the biocompatibility of PC-modified films, provide new tools toward the surface modification of biomaterials.

Acknowledgment. The work was supported by research grants from the Canadian Institutes of Health Research, the Natural Sciences and Engineering Research Council of Canada and the FQRNT Centre for Self-Assembled Chemical Structures. The authors thank P. Moraille and J. Sanchez of the Laboratoire de Caractérisation des Matériaux (Université de Montréal) for their help during AFM imaging experiments, L. Norman (Département de Chimie, Université de Montréal) for help with the SPR equipment, and Dr. X.-P. Qiu for his help in the synthesis of PC−CH.

Supporting Information Available. Plots showing fitting of the surface coverage versus number of bilayers and fitting of the QCM data according to the model described in the Materials and Methods section. This material is available free of charge via the Internet at http://pubs.acs.org.

References and Notes

(1) Decher, G. Fuzzy nanoassemblies: Toward layered polymeric multicomposites. *Science* **1996**, *277*, 1232−1237.
(2) *Multilayer Thin Films: Sequential Assembly of Nanocomposite Materials*; Decher, G., Schlenoff, J. B., Eds.; Wiley-VCH: Weinheim, Germany, 2002.
(3) Serizawa, T.; Yamaguchi, M.; Akashi, M. Alternating bioactivity of polymeric layer-by-layer assemblies: Anticoagulation vs procoagulation of human blood. *Biomacromolecules* **2002**, *3*, 724−731.
(4) Thierry, B.; Winnik, F. M.; Merhi, Y.; Silver, J.; Tabrizian, M. Bioactive coatings of endovascular stents based on polyelectrolyte multilayers. *Biomacromolecules* **2003**, *4*, 1564−1571.
(5) Richert, L.; Lavalle, P.; Payan, E.; Shu, X. Z.; Prestwich, G. D.; Stoltz, J.-F.; Schaaf, P.; Voegel, J.-C.; Picart, C. Layer by layer buildup of polysaccharide films: Physical chemistry and cellular adhesion aspects. *Langmuir* **2004**, *20*, 448−458.
(6) Berg, M. C.; Khademhosseini, A.; Yeh, J.; Eng, G.; Cheng, J.; Farokhzad, O. C.; Langer, R. Micropatterned cell co-cultures using layer-by-layer deposition of extracellular matrix components. *Biomaterials* **2006**, *27*, 1479−1486.
(7) van den Beucken, J. J. J. P.; Vos, M. R. J.; Thune, P. C.; Hayakawa, T.; Fukushima, T.; Okahata, Y.; Walboomers, X. F.; Sommerdijk, N. A. J. M.; Nolte, R. J. M.; Jansen, J. A. Fabrication, characterization, and biological assessment of multilayered DNA-coatings for biomaterial purposes. *Biomaterials* **2006**, *27*, 691−701.
(8) Georges, P. C.; Janmey, P. A. Cell type-specific response to growth on soft materials. *J. Appl. Physiol.* **2005**, *98*, 1547−1553.
(9) Discher, D. E.; Janmey, P.; Wang, Y. L. Tissue cells feel and respond to the stiffness of their substrate. *Science* **2005**, *310*, 1139−1143.
(10) Mermut, O.; Lefebvre, J.; Gray, D. G.; Barrett, C. J. Structural and mechanical properties of polyelectrolyte multilayer films studied by AFM. *Macromolecules* **2003**, *36*, 8819−8824.
(11) Pavoor, P. V.; Bellare, A.; Strom, A.; Yang, D.; Cohen, R. E. Mechanical characterization of polyelectrolyte multilayers using quasi-static nanoindentation. *Macromolecules* **2004**, *37*, 4865−4871.
(12) Richert, L.; Engler, A. J.; Discher, D. E.; Picart, C. Elasticity of native and cross-linked polyelectrolyte multilayer films. *Biomacromolecules* **2004**, *5*, 1098−1116.
(13) Nolte, A. J.; Rubner, M. F.; Cohen, R. E. Determining the Young's modulus of polyelectrolyte multilayer films via stress-induced mechanical buckling instabilities. *Macromolecules* **2005**, *38*, 5367−5370.
(14) Collin, D.; Lavalle, P.; Garza, J. M.; Voegel, J.-C.; Schaaf, P.; Martinoty, P. Mechanical properties of cross-linked hyaluronic acid/poly-(L-lysine) multilayer films. *Macromolecules* **2004**, *37*, 10195−10198.
(15) Jaber, J. A.; Schlenoff, J. B. Dynamic viscoelasticity in polyelectrolyte multilayers: Nanodamping. *Chem. Mater.* **2006**, *18*, 5768−5773.
(16) Picart, C.; Sengupta, K.; Schilling, J.; Maurstad, G.; Ladam, G.; Bausch, A. R.; Sackmann, E. Microinterferometric study of the structure, interfacial potential, and viscoelastic properties of polyelectrolyte multilayer films on a planar substrate. *J. Phys. Chem. B* **2004**, *108*, 7196−7205.
(17) Notley, S. M.; Eriksson, M.; Wagberg, L. Visco-elastic and adhesive properties of adsorbed polyelectrolyte multilayers determined in situ with QCM-D and AFM measurements. *J. Colloid Interface Sci.* **2005**, *292*, 29−37.
(18) Salomäki, M.; Laiho, T.; Kankare, J. Counteranion-controlled properties of polyelectrolyte multilayers. *Macromolecules* **2004**, *37*, 9585−9590.
(19) Salomäki, M.; Kankare, J. Modeling the growth processes of polyelectrolyte multilayers using a quartz crystal resonator. *J. Phys. Chem. B* **2007**, *111*, 8509−8519.
(20) Boulmedais, F.; Bozonnet, M.; Schwinté, P.; Voegel, J.-C.; Schaaf, P. Multilayered polypeptide films: Secondary structures and effect of various stresses. *Langmuir* **2003**, *19*, 9873−9882.
(21) Halthur, T. J.; Elofsson, U. M. Multilayers of charged polypeptides as studied by in situ ellipsometry and quartz crystal microbalance with dissipation. *Langmuir* **2004**, *20*, 1739−1745.
(22) Izumrudov, V. A.; Kharlampieva, E.; Sukhishvili, S. A. Multilayers of a globular protein and a weak polyacid: Role of polyacid ionization in growth and decomposition in salt solutions. *Biomacromolecules* **2005**, *6*, 1782−1788.
(23) Johansson, J. Å.; Halthur, T.; Herranen, M.; Söderberg, L.; Elofsson, U.; Hilborn, J. Build-up of collagen and hyaluronic acid polyelectrolyte multilayers. *Biomacromolecules* **2005**, *6*, 1353−1359.

(24) Thierry, B.; Winnik, F. M.; Merhi, Y.; Tabrizian, M. Nanocoatings onto arteries via layer-by-layer deposition: Toward the in vivo repair of damaged blood vessels. *J. Am. Chem. Soc.* **2003**, *125*, 7494−7495.
(25) Thierry, B.; Kujawa, P.; Tkaczyk, C.; Winnik, F. M.; Bilodeau, L.; Tabrizian, M. Delivery platform for hydrophobic drugs: Prodrug approach combined with self-assembled multilayers. *J. Am. Chem. Soc.* **2005**, *127*, 1626−1627.
(26) Etienne, O.; Schneider, A.; Taddei, C.; Richert, L.; Schaaf, P.; Voegel, J.-C.; Egles, C.; Picart, C. Degradability of polysaccharides multilayer films in the oral environment: An in vitro and in vivo study. *Biomacromolecules* **2005**, *6*, 726−733.
(27) Kujawa, P.; Moraille, P.; Sanchez, J.; Badia, A.; Winnik, F. M. Effect of molecular weight on the exponential growth and morphology of hyaluronan/chitosan multilayers: A surface plasmon resonance spectroscopy and atomic force microscopy investigation. *J. Am. Chem. Soc.* **2005**, *127*, 9224−9334.
(28) Croll, T. I.; O'Connor, A. J.; Stevens, G. W.; Cooper-White, J. J. A blank slate? Layer-by-layer deposition of hyaluronic acid and chitosan onto various surfaces. *Biomacromolecules* **2006**, *7*, 1610−1622.
(29) Lu, H.; Hu, N. Loading behavior of {chitosan/hyaluronic acid}$_n$ layer-by-layer assembly films toward myoglobin: An electrochemical study. *J. Phys. Chem. B* **2006**, *110*, 23710−23718.
(30) Kujawa, P.; Sanchez, J.; Badia, A.; Winnik, F. M. Probing the stability of biocompatible sodium hyaluronate/chitosan nanocoatings against changes in salinity and pH. *J. Nanosci. Nanotechnol.* **2006**, *6*, 1565−1574.
(31) Morra, M. Engineering of biomaterials surfaces by hyaluronan. *Biomacromolecules* **2005**, *6*, 1205−1223.
(32) Toole, B. P. Hyaluronan: From extracellular glue to pericellular cue. *Nat. Rev. Cancer* **2004**, *4*, 528−539.
(33) Kumar, M.; Muzzarelli, R. A. A.; Muzzarelli, C.; Sashiwa, H.; Domb, A. J. Chitosan chemistry and pharmaceutical perspectives. *Chem. Rev.* **2004**, *104*, 6017−6084.
(34) Tiera, M. J.; Qiu, X.-P.; Bechaouch, S.; Shi, Q.; Fernandes, J. C.; Winnik, F. M. Synthesis and characterization of phosphorylcholine-substituted chitosans soluble in physiological pH conditions. *Biomacromolecules* **2006**, *7*, 3151−3156.
(35) Sawada, S.; Sakaki, S.; Iwasaki, Y.; Nakabayashi, N.; Ishihara, K. Suppression of the inflammatory response from adherent cells on phospholipid polymers. *J. Biomed. Mater. Res., Part A* **2003**, *64*, 411−416.
(36) Whelan, D. M.; van der Giessen, W. J.; Krabbendam, S. C.; van Vliet, E. A.; Verdouw, P. D.; Serruys, P. W.; van Beusekom, H. M. M. Biocompatibility of phosphorylcholine coated stents in normal porcine coronary arteries. *Heart* **2000**, *83*, 338−345.
(37) Lavertu, M.; Xia, Z.; Serreqi, A. N.; Berrada, M.; Rodrigues, A.; Wang, D.; Buschmann, M. D.; Gupta, A. A validated ^{1}H NMR method for the determination of the degree of deacetylation of chitosan. *J. Pharm. Biomed. Anal.* **2003**, *32*, 1149−1158.
(38) Kambhampati, D. K.; Knoll, W. Surface-plasmon optical techniques. *Curr. Opin. Colloid Interface Sci.* **1999**, *4*, 273−280.
(39) Martin, S. J.; Granstaff, V. E.; Frye, G. C. Characterization of a quartz crystal microbalance with simultaneous mass and liquid loading. *Anal. Chem.* **1991**, *63*, 2272−2281.
(40) Bandey, H. L.; Martin, S. J.; Cernosek, R. W.; Hillman, A. R. Modeling the responses of thickness-shear mode resonators under various loading conditions. *Anal. Chem.* **1999**, *71*, 2205−2214.
(41) Bund, A.; Chmiel, H.; Schwitzgebel, G. Determination of the complex shear modulus of polymer solutions with piezoelectric resonators. *Phys. Chem. Chem. Phys.* **1999**, *1*, 3933−3938.
(42) Höök, F.; Kasemo, B.; Nylander, T.; Fant, C.; Sott, K.; Elwing, H. Variations in coupled water, viscoelastic properties and film thickness of a Mefp-1 protein film during adsorption and crosslinking: a quartz crystal microbalance with dissipation monitoring, ellipsometry, and surface plasmon resonance study. *Anal. Chem.* **2001**, *73*, 5796−5804.
(43) Lubarsky, G. V.; Davidson, M. R.; Bradley, R. H. Hydration−dehydration of adsorbed protein films studied by AFM and QCM. *Biosens. Bioelectron.* **2007**, *22*, 1275−1281.
(44) Laschitsch, A.; Menges, B.; Johannsmann, D. Simultaneous determination of optical and acoustic thicknesses of protein layers using surface plasmon resonance spectroscopy and quartz crystal microweighing. *Appl. Phys. Lett.* **2000**, *77*, 2252−2254.
(45) Salomäki, M.; Vinokurov, I. A.; Kankare, J. Effect of temperature on the buildup of polyelectrolyte multilayers. *Langmuir* **2005**, *21*, 11232−11240.

BM7006339